On the design of a multi-channel NIR system to monitor functional brain activity.

R. K. Almajidy[a,b], U. G. Hofmann[a,b]

[a] *Institute for Signal Processing, University of Luebeck, Luebeck, Germany*
[b] *Neuroelectronic Systems, Clinic for Neurosurgery, University of Freiburg Medical Center, Freiburg,*

Corresponding author: almajidy@isip.uni-luebeck.de

Introduction

Multi-channel near-infrared spectroscopy (NIRS) offers the potential to substitute, or at least complement, electro-encephalography (EEG) to detect functional activity e.g., in the motor area of the brain. Bedside NIR sensors have been used to investigate the haemodynamic shift caused by specific brain activity, such as epileptic seizures (Watanabe et al., 2000). Although it is clearly a promising data acquisition method, several open issues remain i.e. some NIR systems toggle sequentially through measurement channels, which leads to a slower acquisition time (Bunce et al., 2006). Another issue is caused by unaccounted signal contributions from superficial blood vessels within the scalp and skull. This may dilute the significance of NIR data obtained e.g. when measuring specific regional oxygenation levels during a mental or physical task. In order to investigate both effects, the following study presents the design of a multichannel NIR system that is able to perform both sequential and channel-interleaved signal acquisition. At the same time, we used two NIR detectors per measuring channel to separate the scalp and skull effects (Gersten et al., 2012; Schepens and Waanders, 2008). In order to thoroughly test this NIR system, we improved on an optical brain tissue phantom introduced by Kashyap (2007).

Using such a phantom in the design cycle facilitates optimisation before bringing it to patients.

Materials and Methods

NIR light emitted into the brain can be expected to follow a curved path (Okada, 2000). A photodiode (PD) further away will thus be able to detect backscattered light from a longer path, as compared to a nearby PD, with the consequence of considerably decreased signal amplitude (Denault et al., 2007). A graphic illustration of those two light paths, given a common source, resembles a sickle-shaped area. Thus, the light signal collected by a more distant PD accounts for deeper, more distant brain structures than a closer PD. In situ, a closer diode's signal will be a mixture of the skin, skull and superficial brain's light scattering. It is part of this study to find an estimate of a probable measuring depth at a given LED-PD separation. Consequently, our NIR design is set up using two, four-sensor modules with each sensor consisting of two closely-mounted light emitting diodes (LEDs) in line with two separated PDs (see Figure 1 bottom). Each sensor's PDs are mounted on a flexible printed circuit board (PCB) at two different distances from the light source. One is mounted at a distance of 28 mm and the other at 40 mm. Thus, eight PDs of each module are supposedly measuring light passing through the shallow region of scalp and skull by a shorter source-sensor distance (SSD) and eight are measuring light from deeper regions, presumably from the brain cortex, by a longer SSD during the same measurement. In this way, the scalp and skull contributions to the sensor's signal can be minimised by subtractive design (Schepens and Waanders, 2008).

Since our area of interest lies bilaterally within the cortex motor areas (Coyle et al., 2007), each module's four sensors are oriented in a star shape, thus providing one common area in the cross-section of all light paths (see Figure1 centre). This study's sensor array was designed for detecting the haemodynamic activity in an area of interest, especially the brain area responsible for hand motion (Coyle et al., 2007). The specific differences in absorption spectra of oxygenated (Hb_{ox}) and deoxygenated (Hb_{deox}) haemoglobin enable the determination of blood oxygenation levels by using at least two measuring wavelengths separated by haemoglobin's isosbestic point (Baykut et al., 2001). A similar approach is used in pulsed oximetry, which is commonly used in clinical settings (Kamat, 2002). Based on these considerations, each of our array's NIR sensors consists of two LEDs with wavelengths of 770nm and 850nm and two PDs located 2.8 cm and 4 cm away from the LEDs (Figure 1).

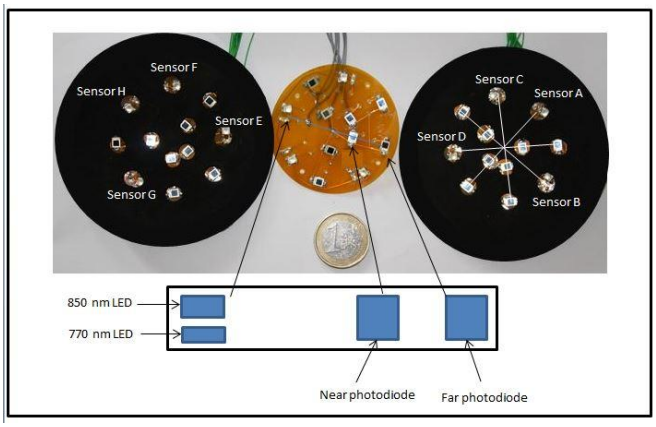

Figure 1. 8 NIR sensors with 4 sensors for the brain's left hemisphere and 4 sensors for the brain's right hemisphere. NIR LEDs and PDs are soldered on a flexible PCB.

This flexible PCB is covered (except for the LEDs and PDs) with black neoprene to eliminate ambient light and increase the sensor's robustness. The near PD is designed to detect NIR light which passes through the scalp and skull, while the far PD is designed to detect NIR lightwhich passes through the scalp, the skull and the brain.

The multichannel NIR circuit presented (each half-sensor (1 LED and 2 PDs) = 1 channel) is an improvement on a two-channel NIR circuit previously presented by our group (Mohammedani et al., 2010; 2011; Mankodiya et al., 2010). Figure 2 shows the circuit board and a block diagram of the current system. This multichannel NIR circuit design consists of three major parts: constant current sources to guarantee stable performance of the 16 NIR LEDs, a receiving circuit to amplify signals detected by the 16 PDs and multiplexers. The circuit is powered using two standard 9 volt batteries.

The receiving circuit consists of the following parts:

(a) Transimpedance amplifiers (with low capacitance to prevent oscillation) will amplify the signals detected by the PDs;

(b) Differential amplifiers subtract the near PDs' voltage from the far PDs' voltage and amplify the output;

(c) Ambient light cancellation will minimise the effect of the ambient light, and

(d) A band pass filter to block signal frequencies outside the desired range.

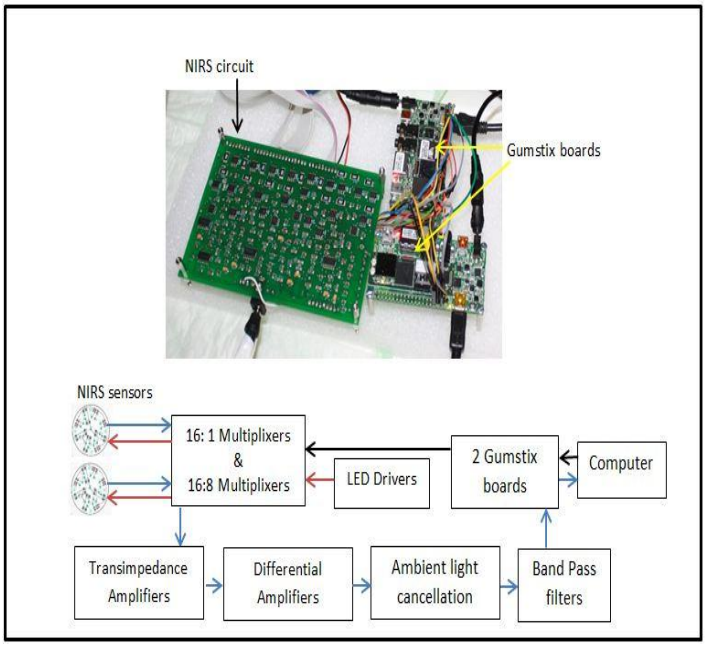

Figure 2. The multichannel NIR circuit board and a block diagram of the system (see text).

The system features two modes for testing purposes. In the first mode, four left and four right hemisphere channels are switched on at the same time (which means faster data acquisition) while in the second mode the channels are sequentially active (which is the regular case). In the first mode, two 16:8 multiplexers are used so that eight LEDs of the same wavelengths (770nm or 850nm) are on at the same time. That way, the circuit receives signals from 16 PDs and produces output for the first 8 channels. Then the other eight LEDs are on and the circuit receives time-delayed signals from the same 16 PDs and produces the output for the second 8 channels. In the second mode, two 16:1 multiplexers are used so that the 16 LEDs operate sequentially while the data is also collected sequentially for each sensor. Two Gumstix Overo Fire on Summit expansion boards (Gumstix Inc.) are used to produce the timing signals for multiplexers, EN and IN for the 16:8 multiplexers (16 Hz and 8 Hz) and EN, IN1, IN2, IN3 and IN4 (16 Hz,8 Hz, 4 Hz,2 Hz,1 Hz) for the 16:1 multiplexers (Figure 3). The NIR circuit output is collected by the both of the Gumstix and then sent to the computer for further analysis.

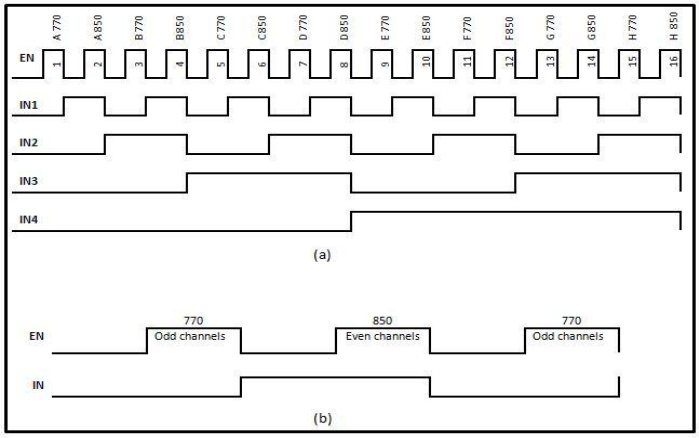

Figure 3. Multiplexer timing signals produced by Gumstix boards and the corresponding NIR circuit operating modes (a) 16:1 multiplexer timing signals. Each half-sensor or channel consists of one LED plus two PDs (near and far). Channels 1, 3, 5, 7, 9, 11, 13 and 15 LEDs are the 770 nm LEDs. Channels 2, 4, 6, 8, 10, 12, 14 and 16 LEDs are the 850 nm LEDs are operating sequentially. (b) 16:8 multiplexer timing signals, 8 channels are operating at the same time.

To validate the system prior to patient contact, a dynamic laboratory brain tissue phantom was used (Figure 4): 28 ml of human blood ware diluted in 1400 ml of Intralipid solution (1% Intralipid in 10x PBS). This solution was filled into two non-concentrically fixed laboratory beakers and continuously stirred using a magnetic stirrer. The inner beaker was used to simulate oxygenation changes in the brain whereas the outer beaker simulated blood vessels within the scalp and skull. Both inner and outer beakers were separately sealed gas-tight using Parafilm and were fixed in relative position by a custom-made base from PLA. The PLA fitting was formed by fused deposit molding with a 3D printer (Makerbot, Replicator2). In order to simulate haemodynamic changes, gas was bubbled through the blood/Intralipid solution in the inner beaker at a rate of ca. 0.5 l/min. Partial deoxygenation was achieved by bubbling nitrogen gas for at least 40 minutes. Due to the high affinity of hemoglobin for O_2, oxygenation took place in a fraction of that time span. We maintained the gas seal by releasing pressure from the inner beaker into a gas trap, water filled beaker (Kashyap, 2007). The "skin-skull phantom" solution was neither de- nor oxygenated but was kept isolated from both inner beaker and ambient air at room temperature (22°-24°). Both NIR left and right sensors (Figure 4) were in good contact with the outer beaker and wrapped firmly to prevent motion during the experiments.

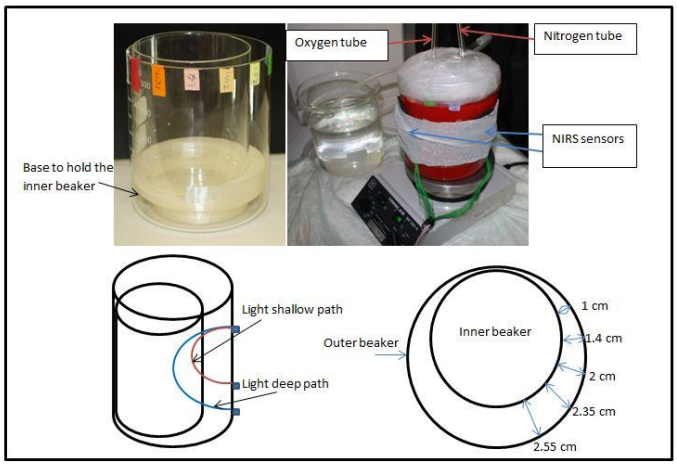

Figure 4. Haemodynamic tissue phantom in two beaker arrangement. Note the top and side view sketches depicting measurement geometry and sensor positioning.

Results and Discussion

Initially the system's design was tested using a one beaker, dynamic brain tissue phantom (Kashyap, 2007). A single-channel voltage output at 770nm is shown in Figure 5. The phantom's solution was deoxygenated for 40 minutes followed by oxygenation for 12 minutes. The increase in PD voltage due to saturation of hemoglobin and subsequent change in absorption parameters due to oxygenation is clearly visible (Fig. 5). The same plot depicts the voltage differences of both the far and the near PD due to path length related signal attenuation.

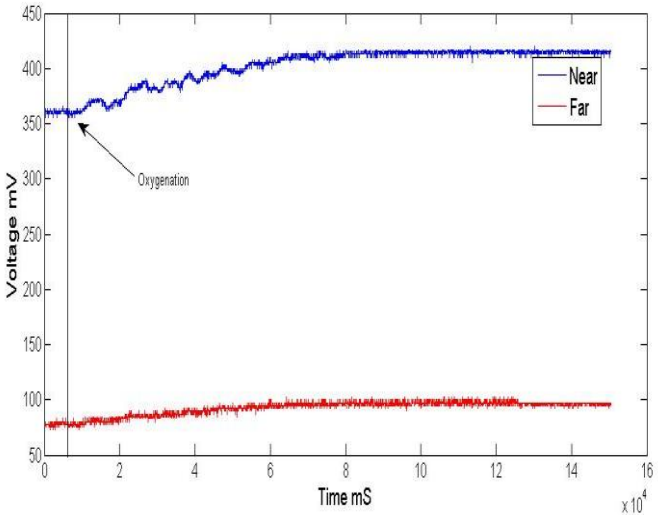

Figure 5. PD signals (near and far diode) at 770nm illumination of a one beaker, phantom upon oxygenation.

In order to get an estimate for the effective measuring depth of our sensor's geometry, we investigated the oxygenation effect of the inner beaker (brain phantom) with different thicknesses of non-oxygenated blood (skin-skull phantom, outer beaker) at one LED wavelength only (770nm). NIRS sensors where placed in various locations around the beaker as shown in Figure 4 and the hemodynamic phantom's inner beaker was partially deoxygenated for 32 minutes and then oxygenated for 10 minutes. To quantify the depth sensitivity, we normalized the voltage differences for the shallow and deep path's photo voltages by the theoretically maximal voltage difference V_{max}. V_{max} is reached, when the entire deep path courses through the oxygenated area only and the entire shallow path never leaves the unaltered blood area.

This is impossible to achieve in our two-beaker geometry, but can be pre-determined sequentially in a one-beaker geometry. Figure 6 shows the normalized differences in photo voltage of the deep and the shallow light path as effect strength with respect to the unaltered blood thickness (outer beaker).

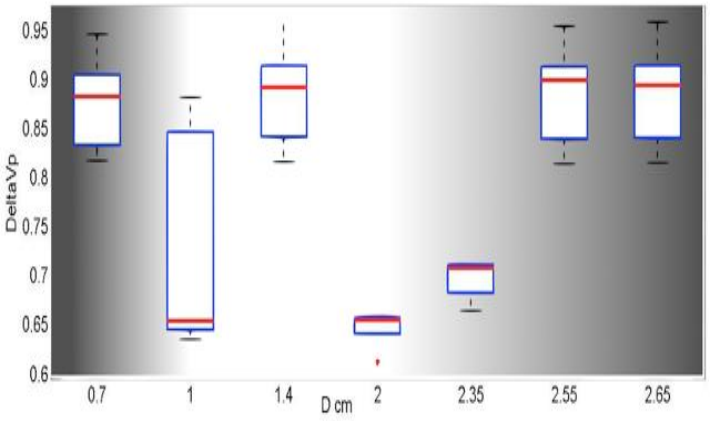

Figure 6. Boxplot of the normalized voltage difference ΔV_p of both PD versus the distance of the sensor to the inner beaker (D cm) during the re-oxygenation.

$\Delta V_p=(V_L-V_s)/V_{max.}$
V_L = Far PD's voltage when the sensor is located at distance D from inner beaker
V_s = Near PD's voltage when the sensor is located at distance D from inner beaker
$V_{max.} = V_{L\,max} - V_{s\,min}$; maximal effect, assuming that the whole long path is in the oxygenated medium and the short path is in the unaltered medium.
$V_{L\,max}$ = Far sensor voltage when the phantom is fully oxygenated
$V_{s\ min}$ = Near sensor voltage when the phantom is fully deoxygenated

Figure 6 illustrates a clear, yet disputable relationship of effect strength over unaltered blood thickness. For a thickness up to 1 cm or above 2.35 cm the normalized voltage difference ΔV_p had similar values. We interpret this fact by having situations where both the shallow and the deep path are coursing through similarly oxygenated medium: For D <1 cm, both paths course mainly through oxygenated medium, whereas for D >2.35 cm both paths course through unaltered blood. This view is supported by one-beaker phantom measurements. For distances between 1 cm and 2.35 cm, however, the deep path runs through oxygenated medium, contributing by higher scattering to an increased deep path photo voltage V_L. It is beyond the scope of this work and a challenge for a simulation study to determine the contributions for each fraction of each scattering path. However, due to unknown peculiarities of the chosen effect quantity ΔV_p, the maximal value within the sensitive depth of 1 to 2.35 cm was found at 1.4 cm depth.
We thus hypothesize for our current geometry that the sensor performance will be best when the distance between the sensor and the origin of a hemodynamic effect will be in the range of 1.4 cm.
When testing the circuit in both operating modes, namely sequential (16:1) and grouped (16:8), the grouped output showed less sensitivity to oxygenation level changes, which is probably due to optical cross talk by LED light from neighboring channels.

Conclusion

The presented novel NIRS system design is based on an embedded dual-core processor running custom made electronics and features the ability to perform high speed NIRS data acquisition targeted on brain (motor) cortex. Subtractive data processing within one sensor at almost the same measuring spot promises to increase signal quality. Using two PDs per NIRS sensor and testing it, using a double-layered brain tissue phantom, will enable us to investigate the optimal SSD to provide signals from the brain with minimum effect from external blood vessels. Bringing both possible LED wavelengths into play (Kamat, 2002), will foster the determination of [HbO_2] in the relatively small brain area involved in controlling hand movement. For this study we did not attempt to go this direction, yet decided to characterize the geometrical and electronic details of our current design. Even though the sensor design produced less accurate data when operating eight channels synchronously and grouped on our beaker phantom, we are confident that a similar design can be used in other locations with a better optical separation of light paths than in a glass beaker.

Acknowledgements

The authors are grateful to Prof. Dr. Rolf Verleger for his valuable suggestions and to Dr. Robert Kirch for his invaluable help, Olaf Christ for designing and printing the beaker base and Abdallah G. Mohammedani for his help in the circuit design. We are grateful to the blood bank of the University Hospital Freiburg for blood samples.

References

Baykut D, Kadipasaoğlu AK, Bölükoglu H, Gebhard MM, Frazier OH, Zerkowski HR (2001). Intravascular detection of ischemia by near-infrared spectroscopy. *Asian Cardiovasc Thorac Ann*. **9**, 296–301.

Bunce SC, Izzetoglu M, Izzetoglu K, Onaral B, Pourrezaei K (2006). Functional near-infrared spectroscopy. *IEEE Eng Med Biol Mag.* **25**, 54-62.

Coyle SM, Ward TE, Markham CM (2007). Brain–computer interface using a simplified functional near-infrared spectroscopy system. *J Neural Eng.* **4**, 219-26.

Denault A, Deschamps A, Murkin JM (2007). A Proposed algorithm for the intraoperative use of cerebral near-infrared spectroscopy. *Semin Cardiothorac Vasc Anesth*. **11**, 274-81.

Gersten A, Perle J, Raz A, Fried R. 2009. Probing brain oxygenation with near infrared spectroscopy (NIRS). *J NeuroQuantology.* **7**, 258-66.

Kamat V (2002). Pulse oximetry. *Indian J Anesth* **46**, 261-8.

Kashyap D (2007). Development of a broadband multi-channel NIRS system for quantifying absolute concentrations of hemoglobin derivatives and reduced scattering coefficients. [PhD thesis]. University of Texas Arlington. 307 pp.

Mankodiya K, Mohammedani AG, Opp A, Gehring H, Klinger M, Hofmann UG (2010). A miniaturized regional cerebral oximeter based on a smartphone processor. Proceedings of the International Biosignal Processing Conference, vol. 109 (pp. 1-3), Berlin, Germany.

Mohammedani AG, Mankodiya K, Opp A, Gehring H, Klinger M, Hofmann UG (2011). An approach to a multiple channel oximetry system. 15th NBC on Biomedical Engineering and Medical Physics, vol. 34 (pp. 89-92). Aalborg, Denmark: IFMBE Proceedings.www.springerlink.com.

Mohammedani AG (2011). Miniaturized oximetry modules for daily-life health monitoring. [MSc Thesis]. University of Luebeck. 81pp.

Okada E (2000). The effect of superficial tissue of the head on spatial sensitivity profiles for near infrared spectroscopy and imaging. *Optical Review.* **7**, 375-82.

Schepens MAAM, Waanders FGJ (2008). Monitoring the brain: Near-infrared spectroscopy. In: Coselli JS, LeMaire SA, Aortic Arch Surgery: Principles, Strategies and Outcomes. (pp. 114-24).Oxford, UK: Wiley-Blackwell Publishing.

Watanabe E, Maki A, Yamashita Y, Koizumi H, Mayanagi Y (2000). Noninvasive cerebral blood volume measurement during seizures using multichannel near infrared spectroscopic topography. *J Biomedical Opt.* **5**, 287-90.